Mergers and ejections of black holes in globular clusters

Sverre J. Aarseth★

Institute of Astronomy, University of Cambridge, Madingley Road, Cambridge CB3 0HA

ABSTRACT

We report on results of fully consistent N-body simulations of globular cluster models with $N = 100\,000$ members containing neutron stars and black holes (BHs). Using the improved 'algorithmic regularization' method of Hellström & Mikkola for compact subsystems, the new code NBODY7 enables for the first time general relativistic coalescence to be achieved for post-Newtonian terms and realistic parameters. Following an early stage of mass segregation, a few BHs form a small dense core which usually leads to the formation of one dominant binary. The subsequent evolution by dynamical shrinkage involves the competing processes of ejection and mergers by radiation energy loss. Unless the binary is ejected, long-lived triple systems often exhibit Kozai cycles with extremely high inner eccentricity ($e > 0.999$) which may terminate in coalescence at a few Schwarzschild radii. A characteristic feature is that ordinary stars as well as BHs and even BH binaries are ejected with high velocities. On the basis of the models studied so far, the results suggest a limited growth of a few remaining stellar mass BHs in globular clusters.

Key words: black hole physics – methods: numerical – globular clusters: general.

1 INTRODUCTION

Recent years have seen many studies relating to the dynamics of black holes (BHs) both in galactic and extragalactic systems. In view of the observations of the S stars at the galactic centre, it is not surprising that most efforts have been directed towards a relatively massive BH. However, there is also considerable interest in the effect of BHs in star clusters. It has been argued that because velocity kicks may occur at formation, some BHs are more likely to be retained in globular rather than open clusters. We may therefore distinguish between problems dealing with several stellar mass BHs or one dominant body formed by an accretion process. As far as N-body simulations are concerned, these two types call for different methods of solution. Thus in the former we need to treat strong interactions of BHs, while in the latter case a number of short binary periods require careful attention. A closer inspection of investigations concerned with a relatively massive BH shows that Newtonian motions are often adopted in full simulations (Brockamp, Baumgardt & Kroupa 2011). On the other hand, investigations involving binary BHs tend to avoid the numerical problems associated with small Schwarzschild radii by artificial scaling of the masses or magnifying the post-Newtonian (PN) effects (Iwasawa, Funato & Makino 2006; Berentzen et al. 2009).

The first full N-body simulation with PN terms (Aarseth 2003b) indicated that a BH binary of intermediate mass may achieve the general relativistic (GR) coalescence condition following eccen-

tricity growth by the Kozai mechanism (Kozai 1962, 2004). This development was made possible by a special integration method for a long-lived massive binary (TTL; Mikkola & Aarseth 2002). An alternative method, suitable for a dominant single BH, showed several examples of GR coalescence for realistic parameters (Aarseth 2007). Although expensive, the so-called wheel–spoke method generalized from a three-body regularization algorithm (Aarseth & Zare 1974; Zare 1974) is accurate and enables extremely close orbits to be studied. It is notable that in both these investigations, Kozai cycles played an important role, with maximum eccentricities often reaching large values (e.g. 0.9999).[1]

The motivation for the present investigation goes back more than 40 years. Thus an early simulation demonstrated that two massive bodies (factor of 5) gave up kinetic energy to the other members and reached the centre after a few crossing times (Aarseth 1971). Since most of the other core particles were expelled, the two dominant members invariably formed a binary. Although the cluster membership was only $N = 250$, the mass segregation still operated in a qualitatively similar way. Given a dynamically shrinking massive binary, the probability of a long-lived triple with suitable inclination is non-negligible, especially since any stellar mass suffices for inducing Kozai cycles.

Further simulations of small globular clusters with $N = 10^5$ members containing a significant BH component were made with

---

[1] Early N-body simulations report large eccentricity growth to $e > 0.999$ at constant semimajor axis in triple systems which exhibit the hallmarks of Kozai cycles (van Albada 1968; Aarseth 1971).

★E-mail: sverre@ast.cam.ac.uk

special-purpose GRAPE computers (Mackey et al. 2008). More recently, similar systems have been studied with graphics processing units (GPUs) which also require special programming (Nitadori 2009). The software implementation in the standard NBODY6 code based on the fourth-order Hermite block-step neighbour scheme has been described in a recent paper (Nitadori & Aarseth 2012). Of special interest here is an application to compact subsystems of more than two dominant members, all of which may be BHs. In particular, we wish to explore possible PN dynamics in a globular cluster context. Although there have been attempts of including the 2.5PN radiation term using the standard NBODY6 code (Aarseth 2003a) by others (Banerjee, Baumgardt & Kroupa 2010), simplified treatments fall short of realistic requirements and hence a fresh approach is called for.

In this paper, we make use of a new powerful integration package that can overcome the main numerical difficulties associated with compact subsystems. Here the challenge is to treat stellar mass BH binaries of extremely short periods during late stages of inspiral using realistic parameters. The improved algorithmic regularization chain method (ARC; Hellström & Mikkola 2010) traces its development from chain regularization (CHAIN; Mikkola & Aarseth 1993) via the logarithmic Hamiltonian method (Mikkola & Tanikawa 1999) and the time-transformed leapfrog code TTL to special treatments of PN terms (Mikkola & Merritt 2008), also denoted algorithmic regularization. The resulting code called NBODY7 is able to deal with extreme few-body configurations up to the final stages of GR coalescence without recourse to artificial scaling of the parameters. A key feature of the present investigation is that velocity kicks are assigned to neutron stars and BHs at formation, such that only about 10 per cent of the membership is retained in both cases. The subsequent evolution by mass segregation of the heaviest members gives rise to compact subsystems which sometimes require PN treatments due to the process of Kozai eccentricity cycles. Consequently, even a small population of stellar mass BHs are able to control the central region. The challenge is then to employ an efficient method for dealing with extremely compact subsystems where PN terms may be needed for the dominant two-body motion.

This paper is organized as follows. We begin by outlining the *N*-body implementation of algorithmic regularization and PN terms for a compact subsystem. Section 3 is devoted to a general description of mass segregation while results for particular models are illustrated in Section 4. Finally, some aspects of the simulations are discussed in Section 5, followed by conclusions.

2 COMPACT SUBSYSTEMS

Simple test calculations with a few free-floating stellar mass BHs added reveal a characteristic behaviour of mass segregation in accordance with expectations. The essential question is concerned with the degree of central concentration, namely when does the innermost core stop shrinking due to binary activity? Some preliminary investigations were sufficiently encouraging to proceed with new code developments as summarized below.

The main challenge for dealing with a compact configuration is to maintain accuracy, albeit at increased cost. This involves some kind of regularization to avoid near-singular force terms. The adopted method (Mikkola & Merritt 2006, 2008) is based on a sophisticated time transformation that enables even collision orbits to be integrated at high accuracy. Briefly, the underlying integrator (Bulirsch & Stoer 1966) senses an approach to collision and avoids evaluating the force at singular points. Moreover, using a judicious choice of coefficients in the time transformation, the problem of large mass

ratios can also be accommodated. Two analogous forms of the time transformations are used for a subsystem of N_{ch} interacting particles (Mikkola & Merritt 2008):

$$\mathrm{d}s = [\alpha(T + B) + \beta\omega + \gamma]\mathrm{d}t = [\alpha U + \beta\Omega + \gamma]\mathrm{d}t, \qquad (1)$$

where d*s* is the new differential time element and α, β, γ are adjustable constants. Furthermore, *T* is the kinetic energy, *U* the (positive) potential energy, *B* the binding energy, $B = U - T$, and Ω is an optional function of the coordinates. It can be shown that this relation provides well-behaved solutions for two-body collisions when used in connection with a simple leapfrog algorithm where the results are improved by an extrapolation method. Moreover, the case of velocity-dependent perturbations (e.g. PN terms) can be treated explicitly with high accuracy (Hellström & Mikkola 2010).

The alternative time transformations are applied to coordinate and velocity leapfrog integrations, respectively. Thus the Ω-formulation is related to the TTL method in which $\dot{\omega} = \boldsymbol{v} \cdot \nabla\Omega$ provides a regular solution for $\omega(t) = \Omega(t)$ (Mikkola & Aarseth 2002). When a range of masses are involved, the choice $(\alpha, \beta, \gamma) = (1.0, 0.001, 0)$ is recommended, where the non-zero value of β yields increased accuracy for any massive bodies. Note that the algorithmic chain regularization actually employs the chain data structure without solving the corresponding equations of motion. This procedure leads to significant reduction of round-off errors and therefore plays a key role in the formulation.

The choice of the subsystem membership is to some extent experimental. Thus we must consider the cost of treating a small subsystem by an accurate method where a larger size would also necessitate a greater number of perturbers. Note that the basic integrator performs a large number (~100) of function evaluations per step and hence also requires many coordinate predictions of the perturbers for consistency. Although very generous choices of the perturber number have been used before (Harfst et al. 2008), it has yet to be demonstrated that this is necessary. A careful investigation of the corresponding energy change reveals that the external effect is relatively small for dimensionless perturbations beyond $\gamma_{pert} \sim 10^{-9}$ which is a typical limit for selection (reduced from the earlier value 10^{-7}). Even so, perturber numbers of only three or four are typical in the present simulations with small chain memberships.[2] More problematic are the decisions about when a perturber should be included in the membership and vice versa.

The software package ARC replaces the procedures relating to the CHAIN code, with analogous decision making for the interface connection to the standard NBODY6. Consequently, the new code is called NBODY7. Although ARC contains PN terms up to 3.5PN, an alternative formulation up to 3PN (Blanchet & Iyer 2003; Mora & Will 2004) has been retained (Aarseth 2007). This has the advantage that relativistic expressions for the semimajor axis and eccentricity are readily available for decision making and data analysis.

We now review some relevant aspects relating to the implementation of PN terms. The equation of dominant two-body motion with $G = 1$ is written as

$$\frac{\mathrm{d}^2\boldsymbol{r}}{\mathrm{d}t^2} = \frac{M}{r^2}\left[(-1 + A)\frac{\boldsymbol{r}}{r} + B\boldsymbol{v}\right], \qquad (2)$$

where $M = m_1 + m_2$ and *A* and *B* represent the PN terms for coordinates and velocities, *r* and *v*, respectively. The perturbing

---

[2] This behaviour is characteristic for a dominant binary.

force then takes the form:

$$P_{GR} = \frac{m_1 m_2}{c^2 r^2} \left[\left(A_1 + \frac{A_2}{c^2} + \frac{A_{5/2}}{c^3} + \frac{A_3}{c^4} \right) \frac{r}{r} \right.$$
$$\left. + \left(B_1 + \frac{B_2}{c^2} + \frac{B_{5/2}}{c^3} + \frac{B_3}{c^4} \right) v \right]. \tag{3}$$

In *N*-body applications, the scaled speed of light is formally given by $c = 3 \times 10^5 / V^*$, with V^* the velocity unit (typically $16 \, \mathrm{km \, s^{-1}}$ here). However, much smaller values are often used by other workers for easing numerical problems. The expansion coefficients in *A*, *B* to sixth order in $1/c$ are obtained from the current formulation. Although the spin term is of order c^{-3}, it has only been used in tests here for the most dominant body (Gopakumar, private communication). One reason for this neglect is that the spin effect depends on the uncertain initial magnitude as well as direction. However, only the radiation term gives rise to energy dissipation.

The time-scale for gravitational radiation (in *N*-body units) is given by the classical expression (Peters 1964):

$$\tau_{GR} = \frac{5}{64} \frac{a^4 c^5}{X(1+X)m_1^3} \frac{(1-e^2)^{7/2}}{g(e)}, \tag{4}$$

where $X = m_2/m_1$ with $m_1 > m_2$ and $g(e)$ a known function of eccentricity ($\simeq 4.5$ for large *e*). In the relativistic regime, the binding energy per unit mass is determined from

$$\epsilon_b = \epsilon_0 + \frac{\epsilon_1}{c^2} + \frac{\epsilon_2}{c^4} + \frac{\epsilon_3}{c^6}, \tag{5}$$

where ϵ_0 is the Newtonian value. This yields the semimajor axis

$$a = -\frac{M}{2\epsilon_b}. \tag{6}$$

Likewise, the eccentricity is obtained via the angular momentum expansion:

$$J = J_0 \left(1 + \frac{f_1}{c^2} + \frac{f_2}{c^4} \right) \tag{7}$$

by

$$e^2 = \left(1 - \frac{J^2}{Ma} \right). \tag{8}$$

The coefficients $\epsilon_1, \epsilon_2, \epsilon_3, f_1, f_2$ are also taken from the literature cited above.

Another useful quantity is the Lenz vector:

$$e = \frac{v \times r \times v}{M} - \frac{r}{r}, \tag{9}$$

which can be used to determine the Einstein (1915) pericentre shift (in radians per orbit):

$$\Delta w = \frac{6\pi M}{c^2 a(1-e^2)}. \tag{10}$$

An effort has been made to maintain a high level of energy conservation. For this purpose, we split the contributions to subsystem energy changes into two parts. Thus the integrated effect of particle perturbations is used to monitor the instantaneous internal energy while additional contributions arising from the PN terms are treated separately. Although only the gravitational radiation is dissipative, the other terms depend on the orbital parameters and therefore need to be included for conservation purposes. Consequently the sum of the internal energy and the accumulated relativistic energy change is added to the standard *N*-body value based on considering the subsystem as a point-mass body.

The question of when to include PN terms is a delicate one. In view of the increasing cost of the higher orders, we have devised a scheme based on efficiency which has proved itself (Aarseth 2007). The basic idea is to delay the PN stage until the radiation time-scale falls below a specified value, e.g. $\tau_{GR} < 500$ or about 30 Myr. At this stage, the first-order precession terms of comparable cost are also activated, especially because a high precession rate may affect any eccentricity growth. The second and third-order terms are then included once the time-scale shrinks to 50 and 1 *N*-body units, respectively. Inspection of actual examples show that once orbital shrinkage begins, a significant acceleration often takes place, boosted by favourable Kozai cycles.

As an additional safeguard, the next order is also activated if the Kozai period (Kiseleva, Eggleton & Mikkola 1998), T_{Kozai}, falls below a certain value. This time-scale can be evaluated for long-lived triple configurations which are often present. The ultimate aim of PN *N*-body simulations is to see whether coalescence can occur for realistic parameters; in this case, stellar mass BHs in globular clusters. Although even smaller two-body separations can be reached with high accuracy, we now define coalescence at four Schwarzschild radii by

$$R_{coal} = \frac{8M}{c^2}. \tag{11}$$

As can be seen from equation (4), the corresponding time-scale becomes extremely small during the final stages.[3]

Termination by coalescence may also be defined at an earlier stage if conditions are favourable. We distinguish between three different cases: (i) $N_{ch} = 2$ with no perturbers and small τ_{GR} (e.g. $\tau_{GR} < 1$); (ii) $a(1-e) < R_{coal}$ during the second or third PN stage; and (iii) $N_{ch} = 3$, $T_{Kozai} > 25$, likewise for small τ_{GR} and large outer pericentre (factor of 100).

At later times it frequently happens that a dominant binary may not have any perturbers and the GR time-scale is large, in which case it is treated in the usual unperturbed two-body approximation, i.e. with the internal motion frozen. A new subsystem is then re-initialized (at the same orbital phase) once a binary perturber is identified, based on several conservative procedures involving relative distances and velocities (Aarseth 2003a).[4]

The ARC system is advanced in a similar way to the standard CHAIN code. Thus, each block-step time interval is treated sequentially before control is returned to the main code which also deals with regularized binaries in a similar manner. A full discussion of the GPU implementation in NBODY6 has been presented elsewhere (Nitadori & Aarseth 2012).

3 MASS SEGREGATION

We have performed a number of *N*-body simulations in order to improve the statistical results of rare events. Equilibrium Plummer models are used with $N = 1 \times 10^5$ particles and an initial mass function (IMF) mostly in the range 50–0.1 $M_\odot$ (Kroupa, Tout & Gilmore 1993) extended into the brown dwarf regime. We adopt standard *N*-body units with $G = 1$, where the total mass and energy are scaled to 1 and $E = -1/4$, respectively, with mean square velocity of 1/2. Physical units are then readily obtained once the length scale (R^* in pc) and mean mass ($\bar{m} = 1/N$ in $M_\odot$) are specified. For most of the present models, $R^* = 1$pc and $\bar{m} = 0.6 \, M_\odot$, with a scaled half-mass radius $r_h \simeq 0.8$ and time-scale conversion factor

---

[3] Typical parameters are $a = 1 \times 10^{-10}$, $c = 2 \times 10^4$, $m_1 = 3 \times 10^{-4}$.
[4] Following initialization, the relative perturbation is typically $<10^{-7}$.

$T^* = 0.06$ Myr. Likewise, the typical velocity scale unit is $V^* \simeq 16$ km s^{-1}. Since the speed of light is traditionally taken as a free parameter in such simulations, we have adopted $c = 18\,000$ for the final models, close to the actual value.

Before presenting results, it may be of interest to consider the justification for the PN implementation in the context of the present parameters. Let us assume an energetic binary, formed by dynamical means with semimajor axis $a_{hard} \simeq 2/N = 2 \times 10^{-5}$ and component masses 20 M$_\odot$. The energy of the massive binary would then represent 1 per cent of the total energy which can be achieved in this type of simulation. Moreover, from previous experience (Aarseth 2007), a maximum eccentricity of 0.999 is often seen. According to equation (4), the corresponding time-scale would be 35 N-body units or 2 Myr which is practically feasible, although it would require a very large number of binary orbits. Moreover, starting the PN sequence at such high eccentricity usually implies the presence of a Kozai cycle which would tend to counteract the decay and hence assist in reducing the actual time interval further.

The full N-body simulations employ the NBODY6 synthetic stellar evolution package (Hurley, Pols & Tout 2000, 2002) which provides information about stellar mass, radius and type as a function of time. Of particular relevance here are the final BH masses (Eldridge & Tout 2004). Thus for an intermediate metallicity of $Z = 0.001$, each model typically yields about 800 neutron stars and 140 BHs. The latter are in the range 3.0–19 M$_\odot$ with an average mass of 8 M$_\odot$. In the absence of a consensus on BH and neutron star velocity kicks at formation, we adopt a conservative approach. Thus the kick distribution is chosen from a Maxwellian with dispersion $2V^* \simeq 32$ km s^{-1} and applied to both populations, which gives a retention of about 10 per cent. As usual with tidal fields, escaping stars are removed at twice the tidal radius, where $r_{tide} \simeq 56$ pc.

The increased velocity dispersion for BHs due to velocity kicks is evident during the time interval of 4–10 Myr, followed by neutron star formation up to 60 Myr. A further stage of escape reduces the populations to about 14 and 40, respectively, with an average BH mass of 9 M$_\odot$ at age 100 Myr. By this time, the mass segregation of BHs is well developed. A typical behaviour is exhibited in Fig. 1 which shows the mean central distance of two populations, each containing 50 pe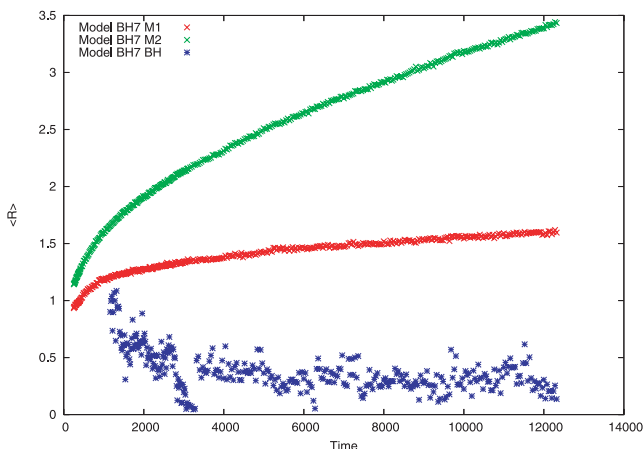r cent of the total mass for Model BH7. The third plot gives the similar information for the BHs. Since the BH membership is relatively small, the geometrical mean separation is used here. This definition is more representative when the result may be affected by a few outliers, including escapers. Unless specified otherwise, all quantities plotted are in N-body units, where the scaling factor for time in Myr is 0.06.

We note the characteristic behaviour that the mean central distance for the heavy members also increases with time.[5] The small BH population exhibits significant contraction subject to sporadic expansion. The rapid expansion of the core from small values ($\simeq 0.05$) near the times 3200 and 6300 is connected with significant binary activity. In fact, the first BH binary is created at the former time ($a \simeq 5 \times 10^{-4}$). Further shrinkage of the expanded core then takes place until a similar minimum is reached whereupon an existing binary experiences exchange with fast ejection ($v_{ej} \simeq 48$ km s^{-1}) of a massive (11 M$_\odot$) component. It is worth noting that already at $t \simeq 3000$ (or 180 Myr) only 14 BHs remain. A third notable event occurs near $t \simeq 9600$ when the binary is ejected in a slingshot interaction from a bound triple. The relative centre of mass (c.m.) velocities of the ejected members, 20 and 63 km s^{-1}, mirror closely the mass ratio of 3.2. Thus we see four distinct stages of core collapse, with only six relatively light BHs remaining when the calculations were terminated.

The GR radiation time-scales of ejected BH binaries are of potential interest for future detectors. In the absence of a systematic study, we note that nearly all the values predicted by equation (4) are well below 10 Gyr with 10–100 Myr being typical, in qualitative agreement with provisional findings (Banerjee et al. 2010).

More pronounced evidence of oscillatory core behaviour can be seen in Fig. 2 which displays the same quantities for Model BH8. Here a genuine GR coalescence occurs near $t \simeq 5060$ but this does not induce core expansion. However, significant binary activity occurs around $t \simeq 5950$ which results in the fast ejection of a massive BH and subsequent expansion. The next noticeable expansion is at $t \simeq 8970$ when a massive triple escaped by the slingshot mechanism. Again the large ejection velocities of 29 and 121 km s^{-1} with respective masses 45 and 11 M$_\odot$ confirm nicely the momentum conservation. It should be emphasized that the slingshot events above were purely Newtonian, with the final transition from $a \simeq 8 \times 10^{-6}$ to 4×10^{-6}.

A comparison between neutron stars and BHs for the last model is shown in Fig. 3, where the mean distance for the neutron stars is also evaluated using the geometric mean. We note the steady trend for the final 41 neutron stars to segregate towards the centre, with only six remaining BHs of mean mass 4 M$_\odot$. Thus, on a slightly longer time-scale the core would be dominated by the neutron stars, nearly all of mass 1.4 M$_\odot$. This difficult and long calculation consumed nearly 300 h, but even so, the accumulated energy error of 7×10^{-5} is highly satisfactory for such a demanding integration. Finally, the general expansion of the whole cluster amounts to a factor of 3 as measured by the half-mass radius, in agreement with a standard calculation (Gieles et al. 2010, equation 6), while the actual binding energy is reduced by 8. Some of the early expansion of the massive component is undoubtedly due to the effects of mass loss from evolving stars. It may also be noted that the mass segregation and formation of a compact subsystem due to dynamical friction is in accordance with earlier theoretical analysis (Spitzer 1969) although a direct comparison would be difficult.

Figure 1. Mean central distance for light masses (upper curve), heavy masses (middle curve) and BHs (lower curve) for Model BH7. Because of mass-loss evolution, the maximum stellar mass has been reduced to 3.1 M$_\odot$ at the end (750 Myr), with the mid-point and lower values at 0.61 and 0.10 M$_\odot$, respectively. A small number of BHs are included in the heavy population but contribute reduced values.

---

[5] The contrast is enhanced further using the geometric mean separation.
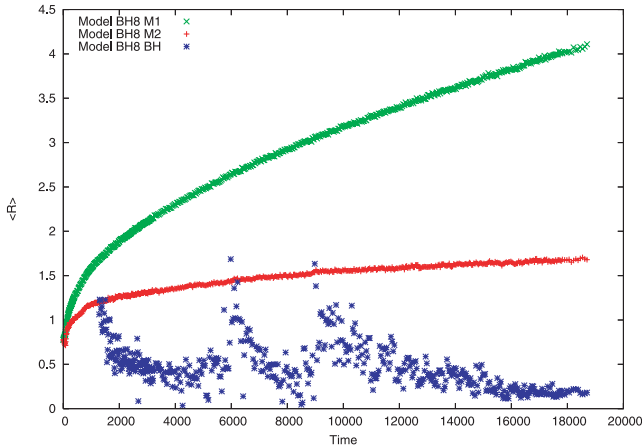
Figure 2. Mean central distance for light masses (upper curve), heavy masses (middle curve) and BHs (lower curve) for Model BH8. The mass ranges are similar to Fig. 1.
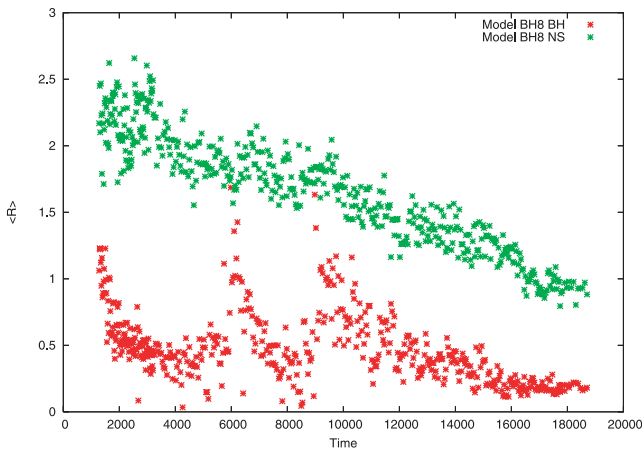

Figure 3. Geometric mean central distance for neutron stars (upper curve) and BHs (lower curve) for Model BH8.

4 MODELS

In this paper, we are mainly interested in the behaviour of BHs. Before looking at detailed results, we summarize some characteristic stages in a selected model displayed below, where i denotes the inclination. Here the key word 'subsystem' means that at least two BHs are sufficiently compact for the new treatment.

(i) BH binary, $t = 465$, $N_{bh} = 9$, $a = 7 \times 10^{-5}$.
(ii) Subsystem, $t = 446$, $a = 3 \times 10^{-5}$, $e = 0.75$.
(iii) Shrinkage, $t = 523$, $a = 1.8 \times 10^{-5}$, $e = 0.65$.
(iv) Kozai cycles, $t = 552$, $i = 98$, $T_{Kozai} = 0.1$ Myr.
(v) Eccentricity, $t = 553$, $a = 8 \times 10^{-6}$, $e = 0.9996$.
(vi) Coalescence, $t = 554$, $a = 1 \times 10^{-11}$, $e = 0.03$.
(vii) Eccentricity, $t = 564$, $a = 3 \times 10^{-4}$, $e = 0.9999$.
(viii) Shrinkage, $t = 638$, $a = 3 \times 10^{-5}$, $e = 0.67$.
(ix) Subsystem, $t = 718$, $a = 2 \times 10^{-5}$, $e = 0.999$.
(x) Coalescence, $t = 720$, $a = 4 \times 10^{-8}$, $\tau_{GR} = 1$.

A few key features in Model BH12 are displayed at different times in Myr. This model is somewhat unusual in that there are two coalescence events, with the most massive BH formed by successive mergers, first by combining 11.9 and 13.4 M$_\odot$, followed by the accretion of 15.6 M$_\odot$. In spite of continuing the calculation another 700 Myr, the massive BH remained in the system because during

this stage the total mass of the other BH members only amounted to 19 M$_\odot$. We note that each coalescence was preceded by high eccentricity which resulted in time-consuming PN calculations until the condition (11) was reached or the time-scale became sufficiently short.

The central concentration of BHs eventually leads to strong interactions. Particularly energetic ejections occur after the formation of a dominant binary and at some stage even the binary may escape due to the recoil effect. All stars with high ejection velocities in Model BH7 are shown in Fig. 4. Here the velocity is evaluated with respect to the subsystem c.m., usually a binary, taking the lower limit of twice the current average velocity which typically ensures escape. In this model, the binary itself was ejected by recoil at time 9600 with velocity $v_{ej} = 20$ km s^{-1} and actual velocity at escape $v_{esc} = 10$ km s^{-1}. There were four other BHs with terminal escape velocity above 20 km s^{-1} but no dynamically ejected neutron stars above half this value.[6] In spite of these strong interactions, the numerical accuracy was maintained well with the accumulated energy error only amounting to 2×10^{-5}. It is also worth noting that the average BH mass declines to about 6 M$_\odot$ which is a direct consequence of mass segregation where the most massive BHs are ejected first.

Although energetic, the ejection of massive binaries invariably occurs using the Newtonian formulation where the semimajor axis is still within a modest factor of a_{hard}. Consequently, favourable configurations are initiated through the Kozai mechanism where eccentricity growth is possible for long-lived triple systems. If a sufficiently large value is reached, the semimajor axis and eccentricity starts decaying according to well-known relativistic expressions (Peters 1964). The subsequent evolution can take several forms, depending on the influence of any perturbers.

Fig. 5 (middle curve) shows the decreasing semimajor axis due to the full PN treatment until coalescence at $a_{coal} \simeq 1.5 \times 10^{-11}$ or 6×10^{-4} R$_\odot$. Note the short time interval corresponding to $\simeq 4 \times 10^3$ yr required for the major part of this inspiral. Also plotted are the orbit-averaged solutions from Peters (1964). Because the initial eccentricity is only available to four significant figures, we have included a trial solution for a possible maximum value (lower curve) which brackets the actual solution. In view of the uncertainty, the qualitative agreement is satisfactory. The late stages of shrinkage are characterized by negligible dynamical perturbations. Nevertheless, in the absence of special procedures, a large number of orbits need to be integrated.

The corresponding plot is shown in Fig. 6 of the maximum eccentricity (Heggie, personal communication). This has been converted to mainly relativistic form[7] and illustrates the role of the Kozai mechanism. In fact, a large value exceeding 0.998 was already reached some 0.4 Myr earlier but the most significant shrinkage took place after the final maximum as well as the actual eccentricity exceeded 0.999. Since the eccentricity did not show any evidence of decrease during the interval, this behaviour is an example of so-called Kozai migration (Wu & Murray 2003). However, the earlier eccentricity maximum would be sufficient to ensure gravitational coalescence on a slightly longer time-scale, provided the favourable configuration is preserved. It can also be seen that the Einstein shift given by equation (10) would still be small during this episode, consistent with the derived value $T_{Kozai} \simeq 1$.

Including all the PN terms up to 3PN demonstrates that the coalescence condition of equation (11) can be reached at the maximum

---

[6] The requirement for parabolic escape is $v_{esc} \simeq 2$ km s^{-1} at $2r_{tide}$.
[7] With two terms of e^2 replaced by relativistic values.

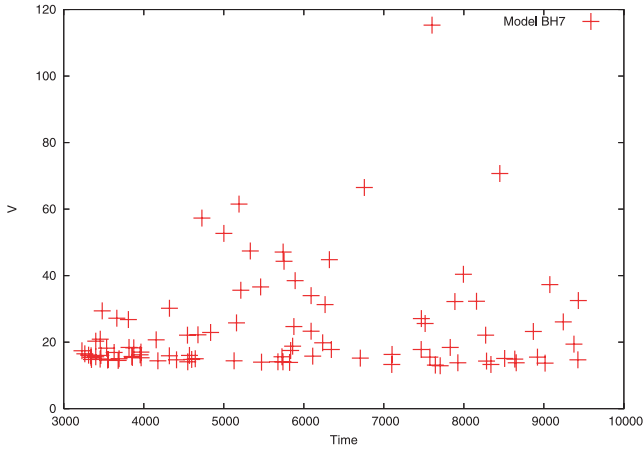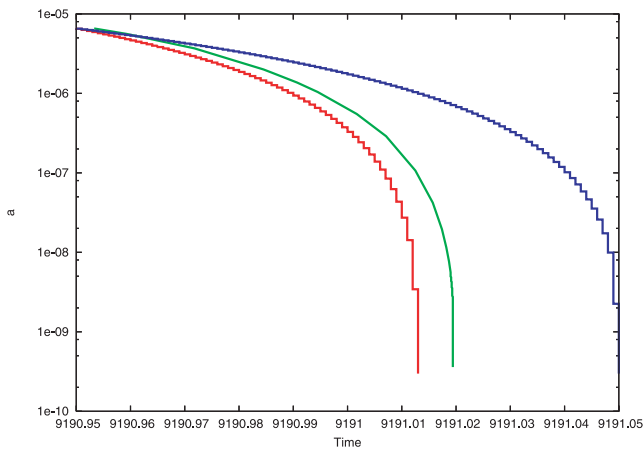**Figure 4.** Ejection velocities in $\mathrm{km\,s^{-1}}$ from the central BH binary for Model BH7.

Figure 5. Semimajor axis as function of *N*-body time. Middle curve: actual plot from Model BH12. Upper and lower curves: orbit-averaged solution from Peters (1964) for two initial values of eccentricity, 0.9996 and 0.99965, where only the four first significant figures are available. The plot is truncated at 3×10^{-10} while the calculation extends to 1.5×10^{-11}.
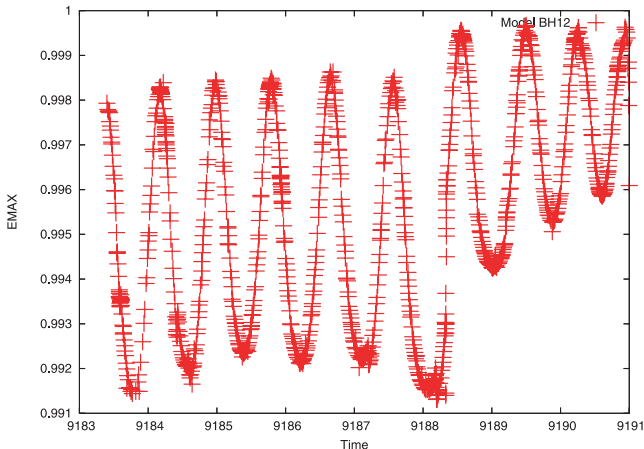

Figure 6. Maximum eccentricity as function of time for Model BH12. Note the late increase of eccentricity due to Kozai cycles.

eccentricity in agreement with estimates of the time-scale (4). This is by no means assured since it is known that the relativistic precession acts to de-tune eccentricity growth. In this connection, a discussion of the PN modification of the Hamiltonian is of interest (Miller & Hamilton 2002). It turns out that the modified expression for the maximum eccentricity still admits values above 0.999 for the parameters of interest here (Aarseth 2007).

A summary of all the coalescence events is given in Table 1. A total of 14 models have been investigated using the PN formulation. However, a few were terminated prematurely because of technical difficulties. Most of the other models were continued further, unless the total BH mass was small. Although all the cases listed were accepted as coalescence, some did not reach the actual end state of equation (11) because one of the secondary criteria discussed above was satisfied. For example, in the case of Model BH11, the eccentricity was extremely large for a short time interval. Likewise, for Model BH14 the high eccentricity and short time-scale would ensure coalescence.

There have been many observational efforts to determine the velocity dispersion as a function of radius, in particular related to the quest for discovering an intermediate-mass BH in a globular cluster. The velocity profiles of all luminous members in two models are shown in Fig. 7 for illustration. Here the more evolved Model BH8 exhibits a larger central velocity, but both models are characterized by a slight velocity decrease in the innermost region. This deficiency

Table 1. Summary of coalescence events. The coalescence time in Myr is given in column 2, followed by the corresponding semimajor axis, eccentricity and combined mass in $\mathrm{M_\odot}$.

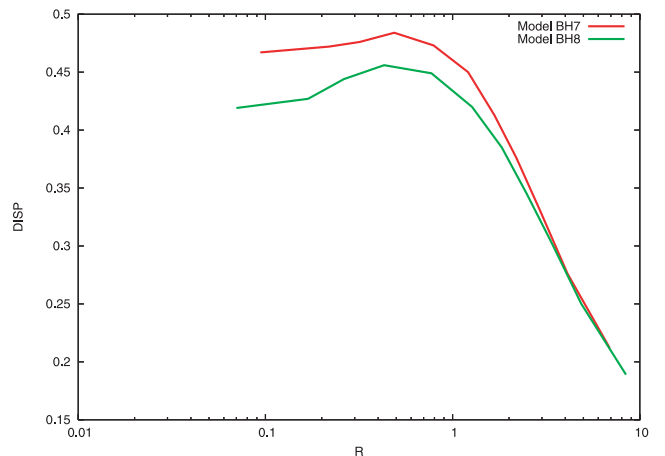| Model	T_{coal}	a	e	m
BH8	300	2×10^{-11}	0.00	35
BH11	184	2×10^{-11}	0.9999	30
BH12	554	1×10^{-11}	0.00	25
BH12	720	4×10^{-08}	0.47	41
BH13	716	3×10^{-07}	0.99	28
BH14	360	6×10^{-07}	0.985	29
BH14	760	2×10^{-06}	0.9997	14

Figure 7. Final velocity dispersion profiles as a function of central distance, Model BH7 (upper curve) and BH8 (lower curve). The current density centre is used as reference point and the respective times are 750 Myr and 1.1 Gyr. BHs and neutron stars have been excluded but the small membership hardly affects the outcome.

may be expected to disappear as the cluster is depleted of BHs. We note that in an investigation involving a population of BHs, the central velocity profile (line of sight) showed a flat slope inside 1 pc (Mackey et al. 2008, fig. 12). However, a direct comparison is difficult because here some 200 BHs were retained.

The density is also of considerable interest. The final densities of the two models shown in Fig. 8 are quite well matched. Consistent with the small velocity decrease towards the centre, the central density profile has a flatter slope. Again this feature will tend to disappear as the post-BH core formation proceeds.

The process of mass segregation plays an important role in the present work. In Fig. 9 we illustrate the average mass as a function of central distance in two typical models where BHs and neutron stars have been excluded. At the end states the maximum mass has been reduced to $3\,M_\odot$ due to stellar evolution, while the minimum mass used is $0.1\,M_\odot$. Although the final times differ somewhat (750 Myr versus 1.1 Gyr), the two plots are essentially indistinguishable and span a significant mass range.

5 DISCUSSION

The main purpose of this paper is to demonstrate the numerical capability of the code NBODY7 for studying strong interactions in cluster cores. It turns out that the algorithmic regularization method is also able to treat PN terms with high accuracy. In fact, energy conservation is now substantially better than in the standard NBODY6 code because the dominant errors are associated with the most strongly bound members and the ARC method is more accurate. This improved treatment comes at a price but already it is feasible to investigate small globular clusters using realistic parameters.

The ARC software usually maintains high accuracy as a result of specifying a small tolerance in the Bulirsch–Stoer integrator combined with a more efficient time transformation. A further advantage compared to standard NBODY6 integration with chain regularization is that the subsystems are treated for much longer times, so there are less errors due to switching. In any case, a direct comparison with the CHAIN code is only possible in the absence of PN terms. Moreover, the latest version of ARC admits solutions with only two members when PN terms are present. It is also helpful that the smaller density in the inner region reduces the energy errors associated with the single particles.
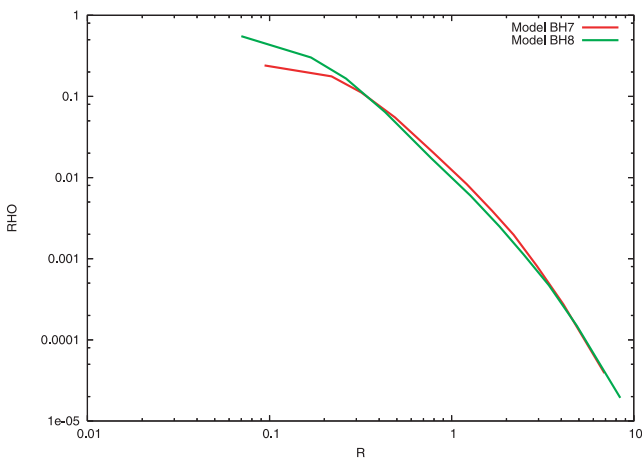

Figure 8. Final density profiles, Model BH7 (upper curve) at 750 Myr and BH8 (lower curve) at 1.1 Gyr. A small number of BHs and neutron stars are included.
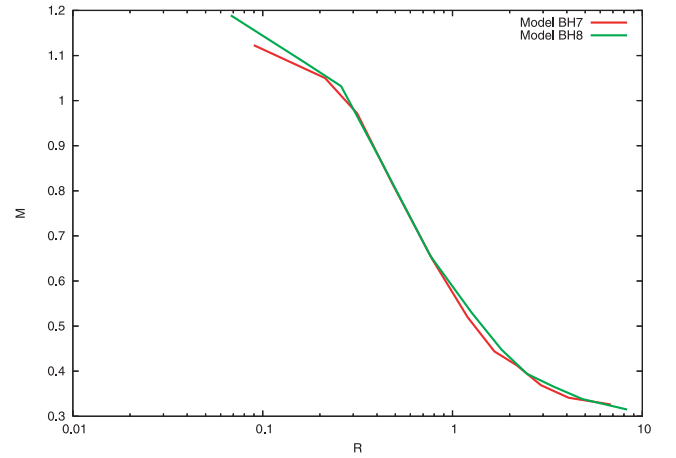

Figure 9. Average stellar mass in solar units as a function of central distance. The plots for Model BH7 at 750 Myr and BH8 at 1.1 Gyr are very similar, with the upper stellar mass limits near $3\,M_\odot$.

The onset of conditions for gravitational radiation is usually initiated by the Kozai mechanism. Following the subsequent shrinkage, the inner binary orbit may become detached (or isolated) so that the final stages are often unperturbed dynamically. This behaviour would enable a sequential analytical continuation of this time-consuming process, taking into account the Einstein shift of equation (10) or the addition of its second-order equivalent.[8]

Stellar systems containing a population of massive objects experience mass segregation on a short time-scale. Although the velocity kick at formation increases the velocity dispersion of neutron stars and BHs, the remaining BHs soon begin to concentrate towards the centre. However, the emergence of a dominant binary acts to deplete the central density and prevents the formation of other binaries, an aspect which has not been considered so far.

The problem of BH dynamics has been studied by many authors. Most studies, however, have been concerned with choices of the IMF which are more applicable to intermediate-mass BHs and hence comparisons are not appropriate. The requirement of realistic PN treatment is also rarely addressed. For these reasons, we only mention one recent work based on stellar mass BHs (Banerjee et al. 2010). Here, an IMF truncated to low-mass stars ($m < 1\,M_\odot$) was adopted with an addition of about 100 BHs of $10\,M_\odot$. Although not a fully consistent simulation, the characteristic behaviour of mass segregation was seen, together with ejection of massive members. Moreover, employment of the relativistic orbit-averaged changes in semimajor axis and eccentricity (Peters 1964) gave rise to several cases of coalescence.

Contrary to the evidence for BH binary formation, a full simulation by NBODY7 with all 140 BHs retained showed that few binaries are formed dynamically during the first Gyr when half the BHs have escaped. This behaviour can be understood in terms of an emerging binary being exposed to disruptive encounters with the dominant binary before becoming hard. There remains the possibility, however, that a dominant binary may be ejected temporarily from the core by recoil, giving the more weakly binary an opportunity of hardening.

The question of BH coalescence by the Kozai mechanism in long-lived triple systems has also been discussed elsewhere (Miller & Hamilton 2002). However, this work assumes a certain fraction of BH binaries in order for binary–binary collisions to take place

---

[8] The analytical continuation procedure has been implemented recently.

and is therefore not consistent with the current findings. Given the relatively small number of BHs expected from a realistic IMF, the potential for massive binary formation is fairly limited. Moreover, the possible depletion due to natal velocity kicks should also be taken into account.

For completeness, a runaway scenario for compact objects was also studied with a full PN formulation (Kupi, Amaro-Seoane & Spurzem 2006). In this early PN application with the code NBODY6++, the treatment of all close two-body encounters was modified by including the effect of relativistic perturbations. Given the large central velocity dispersion of 4300 km s^{-1}, a massive object was formed by runaway accretion after core collapse. We note that the Kustaanheimo & Stiefel (1965) Hermite implementation also requires the first time derivative of the relevant PN force terms, while in algorithmic or chain regularization only the basic expressions of equation (3) are needed.

6 CONCLUSIONS

This is a first *N*-body implementation of the new algorithmic regularization scheme (Hellström & Mikkola 2010). The application to a system containing BHs poses certain numerical problems, mainly in connection with membership selection. Although the PN terms require time-consuming calculations, it has proved possible to describe the full binary evolution up to coalescence using realistic parameters. Further progress can be made taking advantage of analytical continuation of unperturbed binaries in the relativistic regime after allowing for the precession. The question of how to initialize the spin must also be addressed. Its contribution to the PN terms enters at the order c^{-3} and is therefore more important than the 2PN terms.[9] On the observational side, we emphasize the presence of additional escaping stars of high velocity, especially in the later stages when massive stellar binaries are no longer present.

The present results indicate that there is no evidence for runaway evolution of BH masses. Given the relatively small number of BHs involved, just one binary may dominate the central region. Occasionally strong interactions lead to fast ejection of other BHs and even the binary may escape in a slingshot event. These simulations show that even a small number of BHs may play an important role in the first Gyr of globular cluster evolution. Since the simulations only cover the first Gyr so far, later stages may repopulate the core in accordance with expectations. In the absence of a definite model for natal BH velocity kicks, further explorations of larger populations are desirable. We have seen that the Kozai mechanism can be very effective in leading to the relativistic coalescence of BH binaries. As far as stellar mass BHs are concerned, sufficiently high eccentricities can be reached without the growth being de-tuned by precession effects. Finally, the presence of even a few stellar mass BHs with luminous companions may provide a new challenge for future observations.

REFERENCES

Aarseth S. J., 1971, Ap&SS, 13, 324
Aarseth S. J., 2003a, Gravitational N-Body Simulations. Cambridge Univ. Press, Cambridge
Aarseth S. J., 2003b, Ap&SS, 285, 367
Aarseth S. J., 2007, MNRAS, 378, 285
Aarseth S. J., Zare K., 1974, Celest. Mech., 10, 185
Banerjee S., Baumgardt H., Kroupa P., 2010, MNRAS, 402, 371
Berentzen I., Preto M., Berczik P., Merritt D., Spurzem R., 2009, ApJ, 695, 455
Blanchet L., Iyer B., 2003, Classical Quantum Gravity, 20, 755
Brockamp M., Baumgardt H., Kroupa P., 2011, MNRAS, 418, 1308
Bulirsch R., Stoer J., 1966, Numer. Math., 8, 1
Einstein A., 1915, Sitzungsber. Preuss. Acad. Wiss., 47, 2, 831
Eldridge J., Tout C. A., 2004, MNRAS, 353, 87
Gieles M., Baumgardt H., Heggie D. C., Lamers J. G. L. M., 2010, MNRAS, 408, 16
Harfst S., Gualandris A., Merritt D., Mikkola S., 2008, MNRAS, 389, 2
Hellström C., Mikkola S., 2010, Celest. Mech. Dyn. Astron., 106, 143
Hurley J. R., Pols O., Tout C. A., 2000, MNRAS, 315, 543
Hurley J. R., Pols O., Tout C. A., 2002, MNRAS, 329, 897
Iwasawa M., Funato Y., Makino J., 2006, ApJ, 651, 1059
Kiseleva L. G., Eggleton P. P., Mikkola S., 1998, MNRAS, 300, 292
Kozai Y., 1962, AJ, 67, 591
Kozai Y., 2004, Proc. Japan. Acad., Ser. B, 80, 157
Kroupa P., Tout C., Gilmore G., 1993, MNRAS, 262, 545
Kupi G., Amaro-Seoane P., Spurzem R., 2006, MNRAS, 371, L45
Kustaanheimo P., Stiefel E., 1965, J. Reine Angew. Math., 218, 204
Mackey A. D., Wilkinson M. L., Davies M. B., Gilmore G. F., 2008, MNRAS, 386, 65
Mikkola S., Aarseth S. J., 1993, Celest. Mech. Dyn. Astron., 57, 439
Mikkola S., Aarseth S. J., 2002, Celest. Mech. Dyn. Astron., 84, 343
Mikkola S., Merritt D., 2006, MNRAS, 372, 219
Mikkola S., Merritt D., 2008, AJ, 135, 2398
Mikkola S., Tanikawa K., 1999, MNRAS, 310, 745
Miller M. C., Hamilton D. P., 2002, ApJ, 576, 894
Mora T., Will C., 2004, Phys. Rev. D, 69, 104021
Nitadori K., 2009, PhD thesis, University of Tokyo
Nitadori K., Aarseth S. J., 2012, MNRAS, in press
Peters P. C., 1964, Phys. Rev., 136, B1224
Spitzer L., 1969, ApJ, 158, L139
van Albada T. S., 1968, Bull. Astron. Inst. Neth., 19, 479
Wu Y., Murray N., 2003, ApJ, 589, 605
Zare K., 1974, Celest. Mech., 10, 207

---

[9] Spin and a small merger recoil velocity have now been implemented.

This paper has been typeset from a TeX/LaTeX file prepared by the author.